Article

Chinese Science Bulletin

Materials Science

August 2013 Vol.58 No.24: 3033–3042
doi: 10.1007/s11434-013-5874-3

A comparative study of proliferation and osteogenic differentiation of rat adipose-derived stem cells in β-tricalcium phosphate (β-TCP), forsterite (Mg_2SiO_4) and clinoenstatite ($MgSiO_3$)

LENG Bin[1,2†], JIN XiaoGang[3†], LIN QiuXia[2], CHEN Lei[3], WANG Yan[2], DU ZhiYan[2], LIN KaiLi[3], CHANG Jiang[3], GU XiaoMing[1*] & WANG ChangYong[2*]

[1] *Department of Implantology of People's Armed Police General Hospital, Beijing 100039, China;*
[2] *Department of Advanced Interdisciplinary Studies, Institute of Basic Medical Sciences and Tissue Engineering Research Center, Academy of Military Medical Sciences, Beijing 100850, China;*
[3] *State Key Laboratory of High Performance Ceramics and Superfine Microstructure, Shanghai Institute of Ceramics, Chinese Academy of Sciences, Shanghai 200050, China*

Received December 11, 2012; accepted February 21, 2013; published online May 9, 2013

In this study, the effects of forsterite and clinoenstatite powder extracts on the proliferation and osteogenic differentiation of rat adipose-derived stem cells (ASCs) were investigated and compared with the β-tricalcium phosphate (β-TCP) powder extracts. Methylthiazolyldiphenyl-tetrazolium bromide (MTT) assay and live-dead staining were performed to evaluate the viability and proliferation of rat ASCs. Osteogenic differentiation of rat ASCs were assayed by alkaline phosphatase (ALP) staining and ALP activity test. The expression of osteogenic marker genes (alkaline phosphatase (*ALP*), runt related transcription factor 2 (*Runx2*), collagen type Iα1 (*Col1α1*), secreted phosphoprotein1 (*Spp1*, osteopontin), integrin binding sialoprotein (*Ibsp*), bone gla protein (*Bglap*)) were detected by real-time polymerase chain reaction (PCR). The MTT assay and the live-dead staining showed that all the three ceramics possessed good cytocompatibility with rat ASCs. Furthermore, forsterite and clinoenstatite promoted the proliferation of rat ASCs compared with β-TCP. The results of the ALP activity test and the real-time PCR demonstrated that forsterite and clinoenstatite promoted the osteogenic differentiation of rat ASCs. These results suggested that forsterite and clinoenstatite are bioactive ceramics that may be used for preparation of bone tissue engineering (BTE) scaffolds.

forsterite, clinoenstatite, adipose-derived stem cells, osteogenesis, bone, bone tissue engineering

Citation: Leng B, Jin X G, Lin Q X, et al. A comparative study of proliferation and osteogenic differentiation of rat adipose-derived stem cells in β-tricalcium phosphate (β-TCP), forsterite (Mg_2SiO_4) and clinoenstatite ($MgSiO_3$). Chin Sci Bull, 2013, 58: 3033–3042, doi: 10.1007/s11434-013-5874-3

β-Tricalcium phosphate (β-TCP) has been extensively investigated and clinically used as bone substitute materials because of its similar chemical composition to human bone, good cytocompatibility and osteoconductivity [1,2]. However, some disadvantages of β-TCP such as low compressive strength, inappropriate resorption rate [3], low bioactivity and lack of the ability in promoting osteogenic differentiation [4] have also been reported impeding its wide applications in bone regeneration and bone tissue engineering (BTE).

Recently, MgO-SiO_2-based ceramics have attracted increasing interest in BTE [5], because of their ability of releasing soluble ionic products to stimulate proliferation and osteoblastic differentiation of osteoblasts [6], bone marrow stromal cells (BMSCs) [7] and human adipose-derived stem cells (HASCs) [8]. In addition, improved mechanical properties such as fracture toughness, bending strength and Young's modulus of these ceramics have also been observed when compared with β-TCP. It has been reported that akermanite ceramic, a new MgO-SiO_2-based ceramic can enhance the expression of osteogenic marker genes *in vitro*, and promote bone regeneration in rabbit femur defect

† These authors contributed equally to this work.
*Corresponding authors (email: gxmlb@yahoo.cn; wcy2000@yahoo.com.cn)

models with a faster new bone formation rate than β-TCP [9].

Ni et al. [10] and Xie et al. [11] reported a new magnesium-silicate ceramic, forsterite (Mg_2SiO4, M_2S), then demonstrated its good biocompatibility and mechanical properties. Our previous work reported another new magnesium-silicate ceramic, clinoenstatite ($MgSiO_3$, MS), and revealed that the ionic products of the MS powder extracts can promote the proliferation of mouse fibroblasts (L929 cell); and the murine embryonic mesenchymal stem cells adhered well; higher proliferation capacities on the clinoenstatite ceramics were also observed than that on the traditional hydroxyapatite ceramics [12]. These studies suggested that forsterite and clinoenstatite may be the potential and attractive bioactive ceramics for BTE.

As the seed cells for tissue engineering applications, BMSCs have been the subject of considerable researches in BTE over the past 30 years [13,14]. While BMSCs are still a viable option as a stem cell source, however, drawbacks of BMSCs such as painful procedure with possible donor site morbidity, low yield of cell numbers, and difficulties in culture expansion have raising more attentions [15,16]. Recently, adipose-derived stem cells (ASCs) have become an attractive stem cell source with therapeutic applicability in diverse fields for tissues repairment and regeneration [15,17,18]. Combined with a variety of scaffolds, HASCs can form bone in immunodeficient rodent entopic bone models [17,19]. However, similar studies remains rare in rat ASCs [20].

Given the excellent bioactivity of forsterite and clinoenstatite, and the great potential applicability of ASCs for tissue engineering, the purpose of this study was to determine whether forsterite and clinoenstatite can promote the proliferation and osteogenic differentiation of rat ASCs compared with β-TCP. The effects of the three ceramics were evaluated either by culturing cells in ceramic extracts, or by culturing cells on the ceramics disc surface.

1 Materials and methods

1.1 Rat ASCs isolation and culture

All the experiments followed protocols approved by the Animal Care and Use Committee of Academy of Military Medical Science (Beijing, China) and are in compliance with the "Guide for the Care and Use of Laboratory Animals" (National Academy Press, NIH Publication No. 85-23, revised 1996). Male Sprague-Dawley(SD) rats weighing about 100–110 g were purchased from the Experimental Animal Center, Academy of Military Medical Science (Beijing, China).

The adipose tissues were isolated from the subcutaneous inguinal groove of rats and the rat ASCs were isolated according to previous reports [21,22]. Briefly, the adipose tissues were finely minced in phosphate buffered saline (PBS) and digested with 0.1% collagenase IV (Sigma, St. Louis, USA), 0.1% dispase II (Roche Diagnostics, Mannheim, Germany) and 0.05% trypsin (Sigma) in minimum essential medium alpha medium (α-MEM, Gibco, USA) at 37°C for 45 min with gentle agitation. Digestion was neutralized by α-MEM with 10% fetal bovine serum (FBS, Gibco). Neutralized cells were filtered through a 75-μm mesh filter and were centrifuged at 800 × *g* for 6 min. The pelleted stromal cells were resuspended with α-MEM/10% FBS and placed in a 100-mm dish. Adherent cells were cultured in the growth medium (GM, α-MEM/10% FBS) in a humidified 37°C, 5% CO_2 incubator [23]. The primary cells were cultured for 3–5 d until they reached 90% confluence and were passaged at a ratio of 1:3. The cells used in the experiments were between passage 3 and 5. Identification of the rat ASCs was performed by flow cytometry analysis (FCA) with AntiCD90 (Biolegend, San Diego, USA), antiCD29 (Biolegend), antiCD45 (Biolegend), and anti-CD34 (Santa Cruz Biotechnology, Santa Cruz, USA) antibodies.

1.2 Preparation of ceramic extracts

The ceramic extracts were prepared according to previous studies [9]. Briefly, 2 g each of β-TCP, M_2S and MS powder was soaked in 10 mL serum-free α-MEM and incubated in a humidified 37°C, 5% CO_2 incubator for 24 h. The mixture was then centrifuged at 1200 × *g* for 5 min at room temperature, and then the supernatant was sterilized through a filter (Millipore, 0.22 μm) and stored at 4°C (ISO10993-1).

1.3 Preparation of ceramic discs and cell seeding

β-TCP, M_2S and MS ceramic discs with dimensions of 8 mm×0.8 mm were prepared as described previously [8,11,12]. The ceramic discs were sonicated for 5 min, rinsed with distilled water and radiosterilized. Each disc was set in 48-well plate, and was preincubated in the GM for 24 h. The cell suspension was adjusted to a density of 1×10^4 cells/mL, and 1 mL cell suspension was added to each well of 48-well plate and incubated for 12 h.

1.4 Cell proliferation assay

The potential cytotoxicity of the material was assessed by using Methylthiazolyldiphenyl-tetrazolium bromide (MTT) assay (Sigma). To determine the proper concentration of the extracts, a gradient of dilutions was used (200, 100, 50, 25, 12.5, 6.25, 1.25 mg/mL). The rat ASCs were plated (200 μL/well) into 96-well plates at 3×10^3 cells/well and cultured in the GM. After 24 h, the culture medium was replaced by the previously prepared material extracts, using GM without diluted extracts as a negative control. The positive control was prepared with α-MEM/10% FBS supplemented with 10% isolution of oxybenzene. Then cells were cultured for 24, 48, 72, 96, and 144 h. The MTT assay was performed as per the manufacturer's instructions. The optical density (OD)

of each well at 492 nm wavelengths was determined with a microplate reader (Spectra max386plus, Molecular Devices, Sunnyvale, USA). Five specimens for each material were tested for each incubation time.

1.5 Cell viability and proliferation

Cell viability of the rat ASCs cultured in the ceramic extracts was examined after 2 and 4 d in culture, while for cells on the ceramic discs it was tested after 1 and 4 d in culture. Viability was analyzed with a Live-dead Viability Assay Kit (Invitrogen, Paisley, United Kingdom). The cell suspension was adjusted to a density of 1.5×10^4 cells/mL, and 1 mL cell suspension was added to each well of 4-well plate and incubated for 12 h. The culture medium was replaced by GM containing ceramic extracts (20 mg/mL). At each time point, rat ASCs were washed in PBS, then stained concurrently with 4 μmol/L Ethidium homodimer-1 (EthD-1) and 1 μmol/L calcein AM diluted in Dulbecco's Phosphate-Buffered Saline (D-PBS) for 45 min followed by two D-PBS washes to remove excess dye. Live (calceint+) and dead (ETH+) cells were visualized by means of fluorescence microscope.

1.6 Alkaline phosphatase activity assay

Rat ASCs were seeded onto coverslips in 12-well culture dishes (2×10^4 cells/well) and incubated either in GM or osteogenic medium (OM) [9] containing ceramic extracts (20 mg/mL) for 3, 8, and 15 d. ALP staining was performed at each time point using ALP staining kit (Sigma). The coverslips were fixed in citrate buffered acetone (60% acetone and 40% citrate) for 60 s, and rinsed in deionized water for 60 s. Then, they were moved into an alkaline-dye mixture (naphthol AS-MX phosphate alkaline solution-diluted diazonium salt) and incubated at 18–26°C for 60 min in dark. After incubation, the coverslips were rinsed in deionized water for 4 min, and then immersed in hematoxylin solution for 10 min. ALP-positive cells were stained purple.

ALP quantification was also performed as described previously [24]. Cells were seeded onto 24-well culture dishes (1.5×10^4 cells/well) and incubated either in GM or OM for 3, 8, and 15 d. At each time point, cells were treated with 0.2 mL of 0.1% Triton X-100 aqueous solution. The cells then were lysed by freeze-thawing three times. The resulting mixture was then centrifuged at 15000 r/min for 10 min at 4°C. The supernatant was collected, and the activity of ALP was quantified with Wako Lab Assay ALP Kit (Wako Pure Chemical Industries Ltd, Osaka, Japan). Based on the transformation of *p*-nitrophenylphosphate to *p*-nitrophenol (PNP), OD was spectrophotometrically measured at 405 nm as per the manufacturer's instruction. The ALP activity was normalized to the total protein content determined with bicinchonininc acid (BCA) protein assay kit (Solabio, Dalian, China) and expressed as nmol converted PNP/min/mg total protein.

1.7 Quantitative real-time reverse transcription-polymerase chain reaction (RT-PCR) analysis

Total RNA was extracted from cells incubated either in GM or OM containing ceramic extracts (20 mg/mL) on days 3, 8, and 15 by Trizol method. The amount and purity of the RNA samples were determined by optical densitometry at 260 and 280 nm. RNA integrity was confirmed by agarose gel electrophoresis. Complementary DNA (cDNA) was synthesized using cDNA kit (M-MLV, Promega, Madison, USA). Quantitative real-time PCR was performed on Line-Gene Real-Time PCR system (Bori, Hangzhou, China), and SybrGreen PCR MasterMix (Sunbio, Beijing, China) was used in each reaction. Reactions were performed with 40 cycles as follows: 95°C for 20 s, 60°C for 25 s, and 72°C for 30 s. The cDNA was analyzed for the following osteogenic genes: alkaline phosphatase (*ALP*), runt related transcription factor 2 (*Runx2*), collagen typeIα1 (*Col1α1*), secreted phosphoprotein1 (*Spp1*, osteopontin), integrin binding sialoprotein (*Ibsp*), bone gla protein (*Bglap*). Relative expression levels for each gene were normalized to the house keeping gene *β-actin*. Primers for the selected genes are listed in Table 1. Each biological sample was run in technical triplicates for each gene. Blank controls that did not contain cDNA were run in parallel.

1.8 Data analysis

A one-way variance (ANOVA) was conducted to determine whether differences existed among testing groups followed by post hoc analysis. Numerical values were reported as means±SD from three individuals unless otherwise noted, all the analyses were performed by using Chiss 6.0 software. A *P*-value of less than 0.05 was considered statistically significant.

2 Results

2.1 Rat ASCs identification and osteogenic differentiation

Rat ASCs expanded easily in the GM *in vitro* and exhibited a fibroblast-like morphology. Rat ASCs entered a proliferative phase 3–4 d after isolation, and then reached confluence within 48 h (Figure 1(A)). After 21 d of osteogenic induction, microscopic observations showed that the cells appeared polygon and became bigger than the negative control. Von kossa staining and alizarin red S staining was positive for rat ASCs cultured in the OM. Mineral deposition were

Table 1 Sequences of primers

Gene	Primers	GenBank	Amplicon size (bp)
β-actin	F: GGAGATTACTGCCCTGGCTCCTA	NM_031144.2	150
	R: GACTCATCGTACTCCTGCTTGCTG		
ALP	F: CACGTTGACTGTGGTTACTGCTGA	NM_013059.1	158
	R: CCTTGTAACCAGGCCCGTTG		
Runx2	F: CAAGTGGCCAGGTTCAACGA	NM_053470.1	141
	R: GGGACCGTCCACTGTCACTTTAATA		
Col1α1	F: GACATGTTCAGCTTTGTGGACCTC	NM_053304.1	137
	R: AGGGACCCTTAGGCCATTGTG		
Ibsp	F: ATCCGTGCCACTCACTCACTTG	NM_012587.2	191
	R: AGTAGCGTGGCCGGTACTTAAAGA		
Spp1	F: GCCGAGGTGATAGCTTGGCTTA	NM_012881.2	136
	R: GATAGCCTCATCGGACTCCTG		
Bglap	F: TGCAAAGCCCAGCGACTCT	NM_013414.1	159
	R: TTGAGCTCACACACCTCCCTGT		

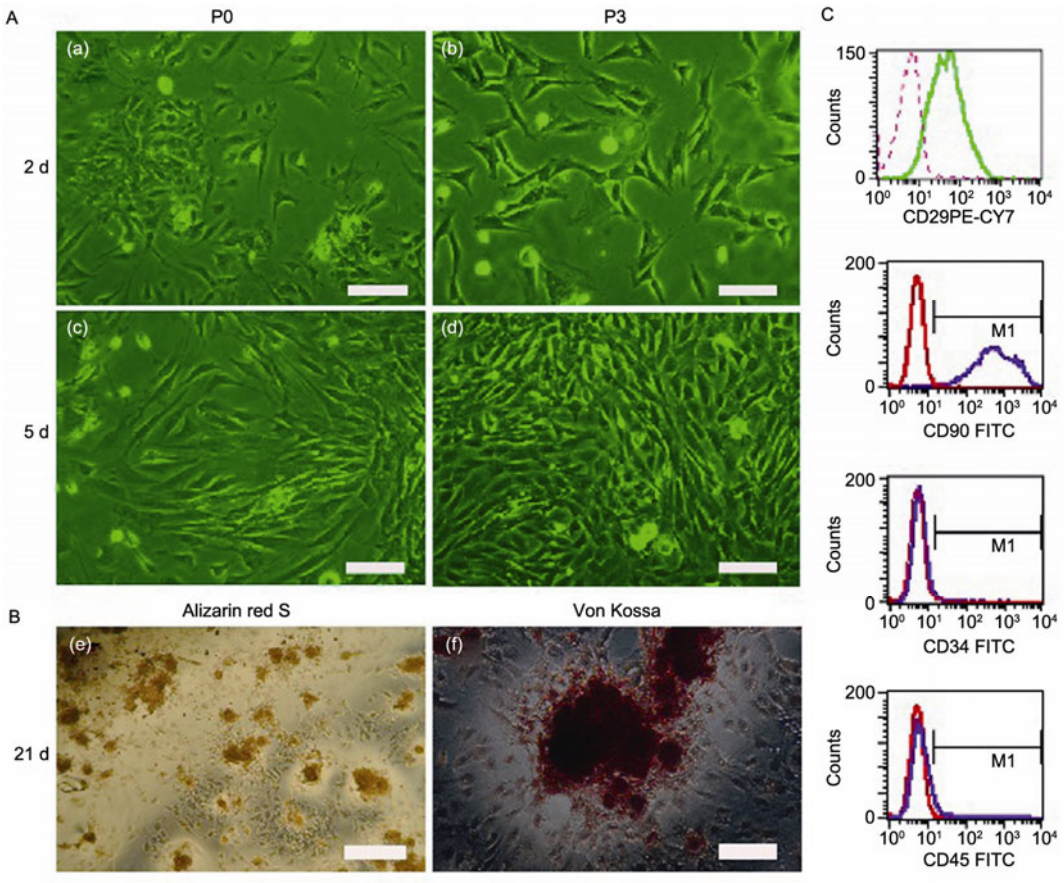

Figure 1 (A) The morphology of cells obtained from adipose tissue in the subcutaneous inguinal groove of SD rats. Primary rat ASCs cultured for 2 d (a) and 5 d (c); passage 3 rat ASCs cultured for 2 d (b) and 5 d (d). Bar scales: 100 μm. (B) Osteogenic differentiation of rat ASCs *in vitro*. alizarin red S staining of the rat ASCs after 21 d osteogenic induction. The red staining represents calcium deposits in the terminal differentiated cells (e); Von Kossa stain of the rat ASCs on day 21 after osteogenic differentiation. The productions of the calcified extracellular matrix strongly suggest mineral deposition around the rat ASCs, forming nodular aggregates (f). Bar scales: 200 μm. (C) Cell-surface marker expression (CD29, CD90, D34 and CD45) in rat ASCs.

observed around the cells forming nodular aggregates under phase contrast microscopy (Figure 1(B)). The flow cytometric surface marker expression analysis of passage 3 cells showed that almost all of the cells were CD29 and CD90 positive but CD34 and CD45 negative (Figure 1(C)).

2.2 Proliferation of rat ASCs cultured with various ceramics extracts

The rat ASCs continually proliferated with culture time in all groups within a certain concentration range (1.25–200

mg/mL) (Figure 2(a) and (b)). The optimal concentrations of the ceramic extracts for cell proliferation are 12.5 mg/mL for MS, and 6.25 mg/mL for β-TCP and M_2S at the time of 96 h after culture (Figure 2(c)). Significantly higher proliferation rates of the cells were observed in the MS and M_2S than that of the cells in β-TCP; the proliferation rates for MS and M_2S groups are 1.68±0.40 and 1.63±0.31 respectively, while that for β-TCP group was 1.30±0.29 (P<0.05) when cells cultured for 96 h with 12.5 mg/mL ceramic extracts (Figure 2(d)).

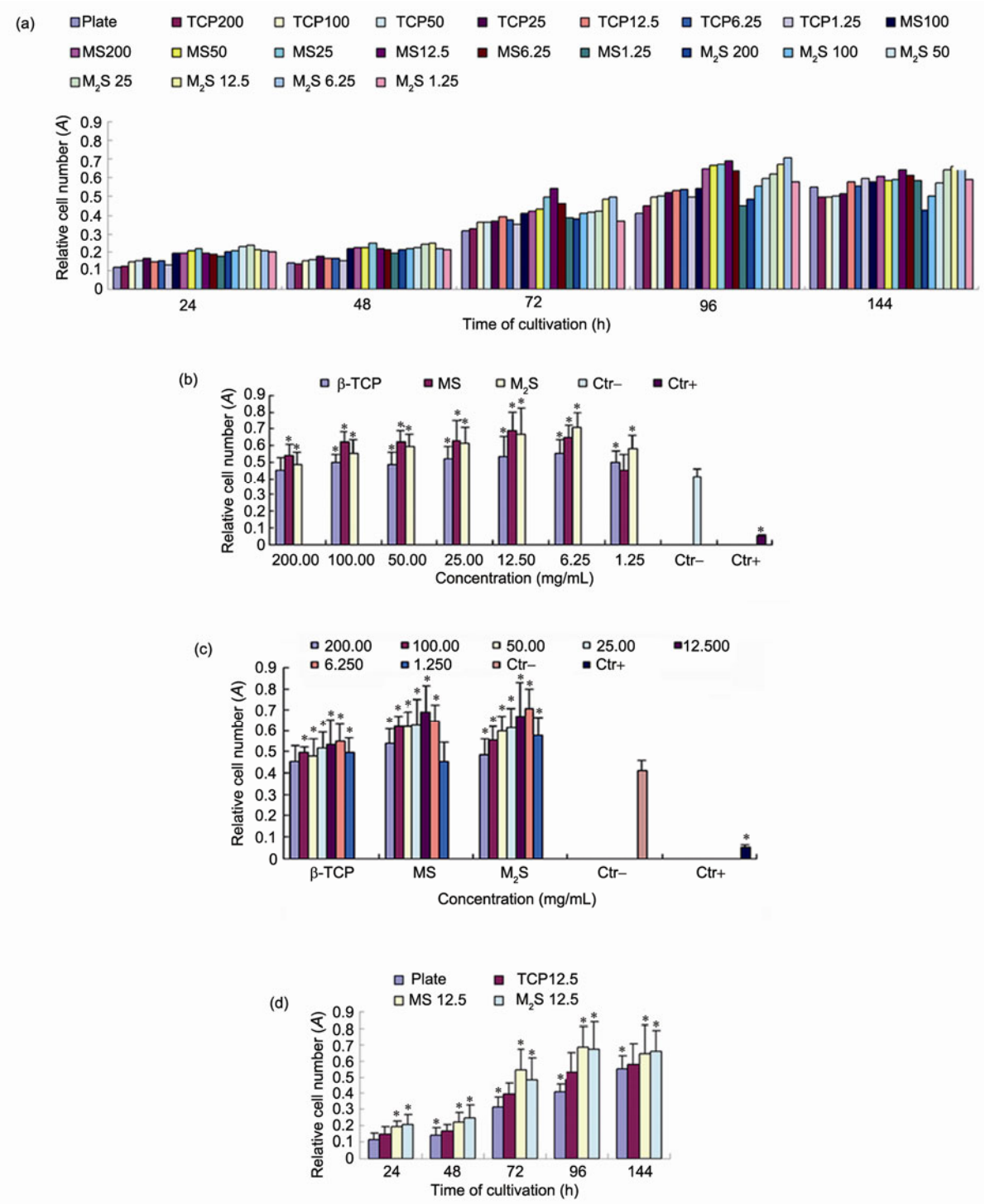

Figure 2 Proliferation of rat ASCs cultured in GM with different concentrations of β-TCP, M_2S and MS extracts at different incubation timepoints (a), in the different concentrations of three ceramic extracts on day 4 after seeding ((b), (c)), and in the concentration (12.5 mg/mL) of the three ceramic extracts at different incubation timepoints (d). The plate in (a) and (d), the Ctr– in (c) all represent the rat ASCs cultured in the GM without any ceramic extracts; Ctr+: positive control (oxybenzene). Results were represented with the means±SD. * means significantly different from the β-TCP group (*P < 0.05).

2.3 Cell viability and proliferation

Less dead cells were observed in M_2S and MS extracts than that in β-TCP on days 2 and 4 after seeding (Figure 3). The cells increased significantly with time, and the proliferation trend of the rat ASCs was consistent with the MTT assay data. Rat ASCs attached and spread well on day 1, and proliferated continually with culture time on all three ceramic discs, especially on the M_2S discs surface (Figure 4).

2.4 ALP activity of rat ASCs cultured in ceramics extracts

Both ALP staining intensities of rat ASCs in ceramics extracts increased gradually with time either in OM or GM, which was consistent with the quantitative assay of ALP. However, no significant difference was found among the three groups at each time point either in OM or GM except for on day 3 in GM (Figure 5).

Quantitative analysis showed that the ALP activity of rat ASCs cultured in all ceramic extracts increased gradually with time either in OM or GM, and the OM enhanced ALP activity compared with the GM at each time point. No significant difference of ALP activity was detected among the three groups in GM on day 3, while significantly different ALP activities were found between M_2S and β-TCP in OM at that time. On day 15 after seeding, significant difference

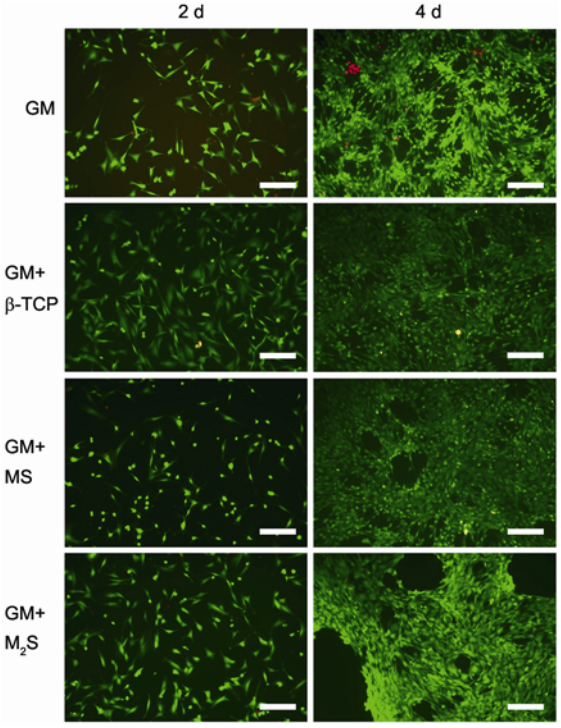

Figure 3 Live-dead staining of the rat ASCs cultured in GM with the concentration (20 mg/mL) of β-TCP, M_2S, and MS extracts on days 2 and 4 after seeding. The viable cells (green fluorescence) and necrotic cells (red fluorescence) were examined by using a fluorescence microscope. Bar scales: 200 μm.

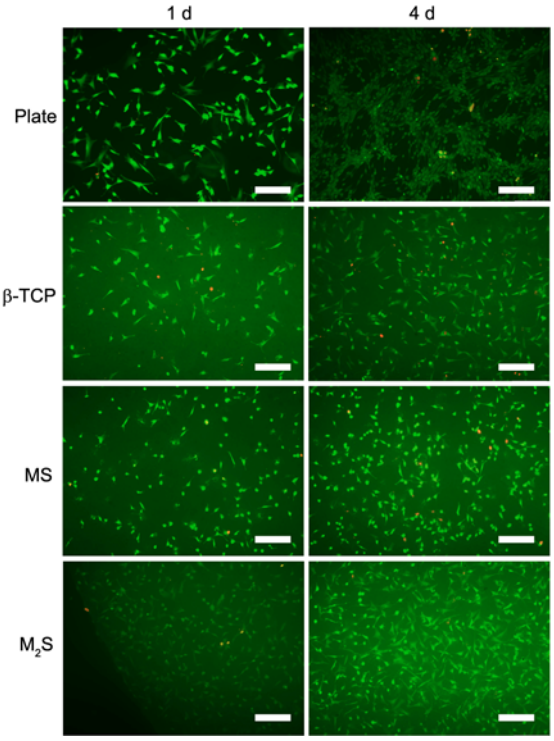

Figure 4 Adhesion and viability assay of rat ASCs cultured on β-TCP, M_2S, and MS ceramic discs. The rat ASCs cultured in 48-well plates at the same seeding density were set as the control. Live-dead staining were performed on days 1 and 4 after seeding. Live cells stained green, while dead cells stained red. Bar scales: 200 μm.

of ALP activity among rat ASCs cultured in three ceramic extracts were detected in either GM or OM. The ALP activity of the rat ASCs in MS and M_2S extracts were considerably higher than that in the β-TCP both in the GM (MS: 109%, M_2S: 124%) and OM (MS: 118%, M_2S: 138%) (Figure 6).

2.5 Osteospecific genes expression of rat ASCs cultured in ceramic extracts

Six osteospecific genes were detected on days 3, 8, 15 after the rat ASCs were cultured in ceramic extracts (20 mg/mL) contained α-MEM. The real-time PCR showed that all the osteospecific genes were unregulated during the culture time. The maximum expression folds of six genes on day15 compared with that of the GM groups on day 3 were as follows: *ALP* (31.7), *Runx2* (24.7), *Col1α1* (8.33), *Spp1* (24.9), *Ibsp* (40.1), *Bglap* (18.8). No significant differences of most gene expression were observed among the three ceramic groups on day 3. After 8 d of culture, the difference of osteogenic gene expression was gradually evident among different groups. After 15 d culture, the expression of *ALP*, *Ibsp* and *Bglap* was significantly higher in M_2S extracts than that in MS extracts. However, the expression of the other three genes such as *Col1α1*, *Runx2*, *Spp1* were higher in MS extracts than that in M_2S extracts. It was noteworthy

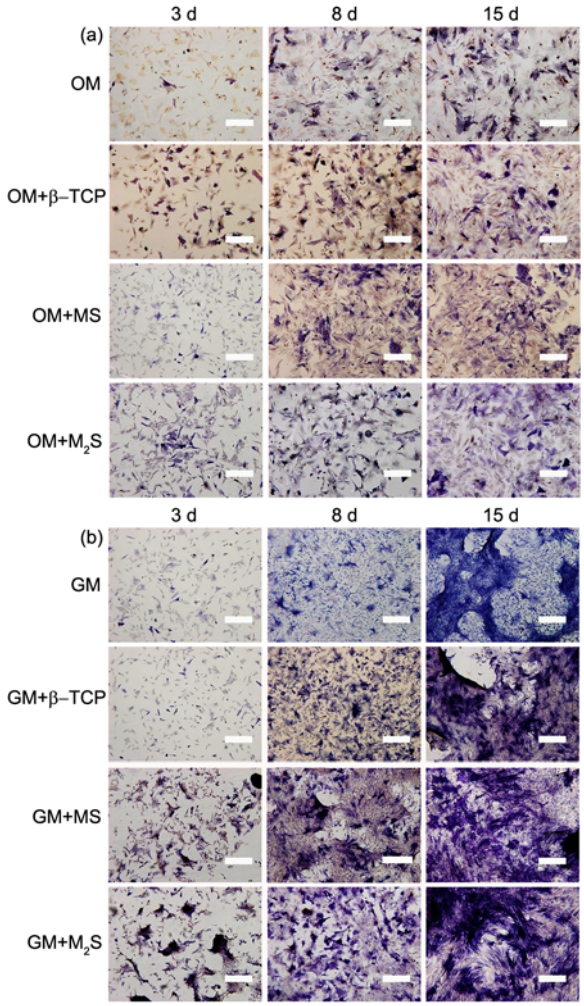

Figure 5 ALP staining of rat ASCs cultured either in OM (a) or GM (b) with ceramic extracts (20 mg/mL) was performed on days 3, 8 and 15 after seeding. ALP-positive cells are shown in purple. Bar scales: 200 μm.

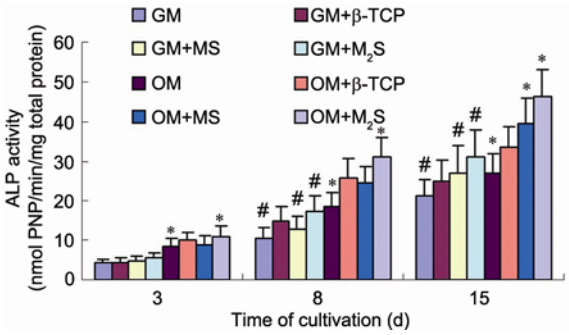

Figure 6 Quantitative ALP activity of rat ASCs cultured in GM or OM with ceramic extracts (20 mg/mL) on days 3, 8 and 15 after seeding. #, $P<0.05$ in GM compared with the β-TCP. *, $P<0.05$ in OM compared with the β-TCP.

that the expression of six osteospecific genes were also detected in the rat ASCs cultured in GM without any ceramic extracts at most of the time points examined in this study (Figure 7).

3 Discussion

The basic strategy of BTE involves the utilization of artificial scaffolds in combination with specific types of cells to repair bone defects structurally and functionally. As an appealing alternative to BMSCs for cell-based BTE, ASCs are been widely using for their abundance, easy accessibility, less invasive operation, easy to amplification and immune-privileged [25,26]. HASCs have rapidly entered into clinical trials for treatment of a broad range of conditions [27–29]. A case undergoing reconstruction of the calvarial defect utilizing ASCs with own cancellous bone and autologous fibrin glue has been reported by Lendeckel [27], while Mesimaki et al. [28] described the first clinical case whose entopic bone was produced using auto ASCs with β-TCP in microvascular reconstruction surgery. However, the reports about rat ASCs as stem cell in BTE is notably less than HASCs [20], so rat ASCs was chosen as stem cell in this study.

Previous studies have showed that magnesium-silicate ceramics could stimulate proliferation and osteoblastic differentiation of osteoblasts, BMSCs and HASCs; in addition, improved mechanical properties of these ceramics were also reported [5–8,30], which suggested that these material may be a potential and attractive bioactive scaffold for BTE. In this study, the effects of two novel magnesium-silicate ceramics (forsterite, clinoenstatite) on the proliferation and osteogenic differentiation of rat ASCs were firstly investigated and compared with that of β-TCP, a ceramic which has been commonly used as bone implant and scaffold in BTE [8].

A suitable scaffold for bone regeneration must be of minor cytotoxicity to allow the survival and proliferation of seeded cells. The present study indicates that both the M_2S and MS posses good cytocompatibility and can even stimulate cell proliferation as compared with β-TCP. Live-dead staining also confirmed that rat ASCs grew well in presence of the three ceramic extracts (20 mg/mL), and less necrotic cells were found in MS and M_2S ceramic extracts than in that of β-TCP (Figure 3). Furthermore, it seems that rat ASCs proliferated more actively in the low concentrations of ceramic extracts than that in the high concentrations. The optimal concentration to promote proliferation of rat ASCs were 12.5 mg/mL for MS, 6.25 mg/mL for M_2S and β-TCP respectively on day 4 post seeding (Figure 2). The results are consistent with that from Kharaziha et al.'s study [31], in which G292 cells were used.

It was reported that akermanite can promote proliferation of HASCs as compared to β-TCP *in vitro* [8]. The Mg and Si ions at certain concentrations dissolved from akermanite ceramics were suggested to be contributive to the enhanced proliferation of HASCs, since Si and Mg have been found in the dissolution of akermanite ceramics, but not in that of β-TCP [6]. Previous studies have shown that, after 1 d

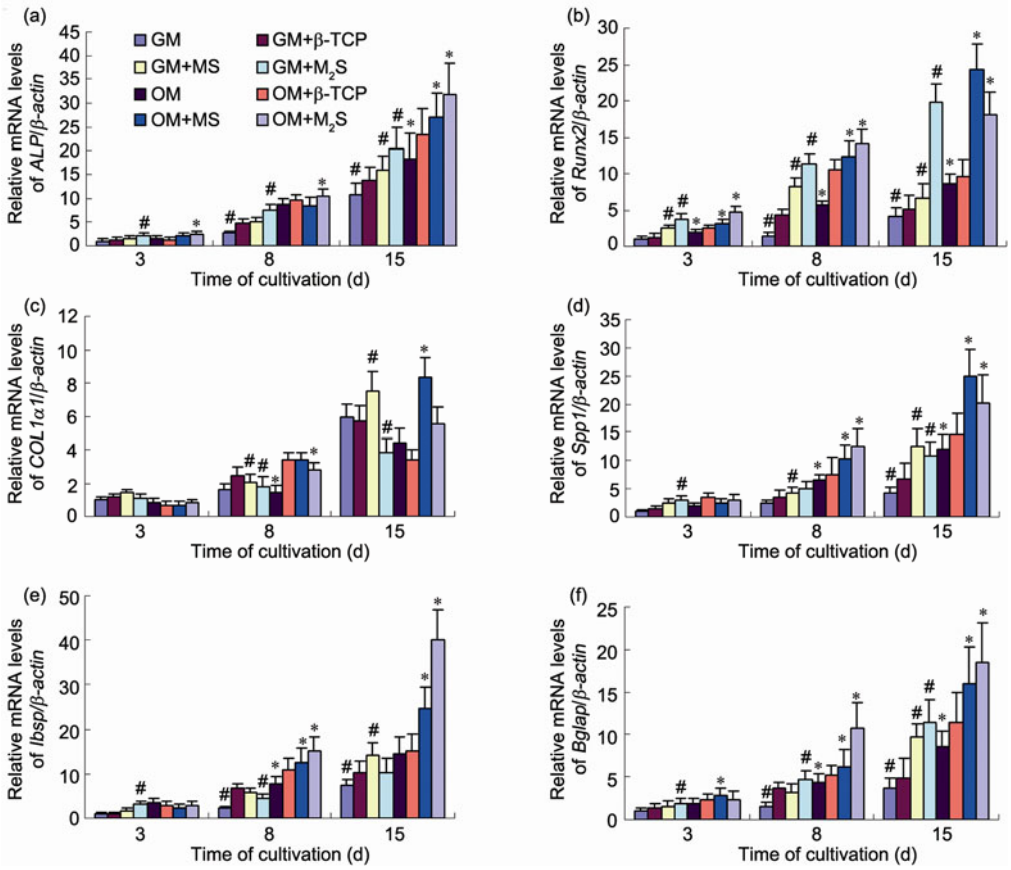

Figure 7 Real-time PCR for 6 osteospecific genes of rat ASCs in GM or OM on days 3, 8, 15. Rat ASCs in GM or OM without ceramic extracts are as control. (a) *ALP*, (b) *Runx2*, (c) *Col1α1*, (d) *Spp1*, (e) *Ibsp*, (f) *Bglap*. #, $P<0.05$ in GM compared with the β-TCP; *, $P<0.05$ in OM compared with the β-TCP.

culture, Mg and Si in the culture medium released from MS and M_2S extracts were 1.67 mmol/L (Mg), 1.97 mmol/L (Si) and 0.65 mmol/L (Mg), 0.23 mmol/L (Si), respectively [11,30]. In this study, the reason of different proliferation rates of rat ASCs in the three ceramics extracts might also be the different ionic concentration of Si and Mg dissolved from the ceramic extracts.

Cellular adhesion to bone substitution materials was considered to play a critical role in the osteointegration and osteoconduction when biomaterials were applied for bone defect repair [32]. In our study, rat ASCs attached well on the three ceramic discs on day 1 after seeding and more cells on M_2S disc were also observed than those on the β-TCP and MS discs on day 4 after seeding, which may indicate the superior ability of M_2S in promoting the proliferation of rat ASCs than β-TCP.

The osteogenic differentiation process of MSCs is characterized by the expression of the osteospecific genes and is typified by extracellular matrix (ECM) mineralization [33,34]. ALP and Runx2 have been considered to be important markers in early stage of osteogenic differentiation [35,36], and Ibsp and Bglap are marker for the late stage of osteoblast maturation [39,40]; Type I collagen are the most abundant structural proteins forming the ECM of bone [37,38], and Spp1 is expressed by pre-osteoblastic cells early in bone formation. In this study, we found that expressions of all these genes were significantly enhanced by the three ceramics; in addition, significantly higher expressions of osteogenic genes were also observed when cells cultured in MS and M_2S compared with β-TCP, which indicated that MS and M_2S may possess a superior capability in promoting osteogenic differentiation of rat ASCs.

Si is an essential trace element involving metabolic processes, which were associated with the development of bone and connective tissues; lots of the silicate-containing ceramics have been proved to be biocompatible and can chemically bond with bone tissue [41]. Mg is closely associated with mineralization of calcined tissues and can indirectly affect mineral metabolism [42,43]. It has been suggested that Mg and Si ions from ceramics contributed to the enhanced proliferation and osteogenic differentiation of MSCs [6,8]. In this study, both MS and M_2S are Si and Mg containing ceramics. Previous studies have showed different concentrations of Mg and Si released from MS and M_2S extracts in the medium[11,30], while no Si or Mg was found in the extracts from β-TCP [6], which may contribute to the different proliferation and osteogenic differentiation rates of rat ASCs with three ceramics extracts in our study. Our

study also revealed that different osteogenic genes were influenced by MS and M_2S extracts as shown in Figure 7, which might be due to their different osteoconductive abilities, different concentrations and Si/Mg ratio in these two ceramics can not be neglected.

The identification of mechanisms that direct adult MSC to osteogenic differentiation is of prime interest for developing therapeutic strategies to promote bone formation and regeneration [44]. Keeting et al. [45] found that Si can enhance osteoblast proliferation, differentiation and collagen production through up-regulation of transforming growth factor beta (TGF-β). Zreiqat et al. [46] found that the cells grown on Mg-riched substrate showed a significantly increased expression of a5β1 integrin receptor and collagen I extracellular matrix proteins. It has been reported that β-TCP scaffold exerts their osteoconductive effects on human osteoblasts through the modulation of a2β1 integrin and mitogen-activated protein kinase (MAPKs)/extracellular regulated kinases (ERK) signaling pathway [47]. Gu et al. [48] found that Ca, Mg and Si ions extracted from akermanite could facilitate the osteogenic differentiation of HASCs via an ERK pathway. In this study, the proliferation and osteogenic differentiation of rat ASCs can be enhanced by MS and M_2S. However, how the ions (Mg and Si) stimulate proliferation and osteogenic differentiation of rat ASCs, and whether Integrins/MAPK/ERK signaling pathway is involved deserved in-depth research.

4 Conclusion

MTT assay found that the proliferation of rat ASCs was enhanced in MS, M_2S powder extracts compared with β-TCP. Live-dead staining confirmed that rat ASCs attached and proliferated well on the M_2S and MS discs as those on β-TCP discs. The real time PCR showed that six osteospecific genes of cells cultured in three ceramic extracts respectively (20 mg/mL) were all upregulated during the culture time. However, the temporal expression patterns were different among the three ceramics. These results suggested that the osteogenic differentiation of rat ASCs could be enhanced when cultured in the MS and M_2S extracts either in GM or OM. Specific environment around the cells caused by the Mg and Si ions released from the ceramics may contribute to these differences among three ceramics in promoting osteogenic differentiation. All the results indicated that forsterite and clinoenstatite ceramics possess good cytocompatibility and osteo-stimulatory activity *in vitro* and may serve as a potential scaffold for BTE applications.

This work was supported by the National Natural Science Foundation of China (*30730034*) *and the National Basic Research Program of China* (*2011CB606206*).

1 Dong J A, Uemura T, Shirasaki Y, et al. Promotion of bone formation using highly pure porous β-TCP combined with bone marrow-derived osteoprogenitor cells. Biomaterials, 2002, 23: 4493–4502
2 Dorozhkin S V, Epple M. Biological and medical significance of calcium phosphates. Angew Chem Int Ed, 2002, 41: 3130–3146
3 Bouler J M, LeGeros R Z, Daculsi G. Biphasic calcium phosphates: Influence of three synthesis parameters on the HA/beta-TCP ratio. J Biomed Mater Res A, 2000, 51: 680–684
4 Miranda P, Pajares A, Saiz E, et al. Mechanical properties of calcium phosphate scaffolds fabricated by robocasting. J Biomed Mater Res A, 2008, 85: 218–227
5 Wu C T, Chang J. Degradation, bioactivity, and cytocompatibility of diopside, akermanite, and bredigite ceramics. J Biomed Mater Res B-Appl Biomater, 2007, 83: 153–160
6 Wu C T, Chang J, Ni S Y, et al. *In vitro* bioactivity of akermanite ceramics. J Biomed Mater Res A, 2006, 76: 73–80
7 Sun H L, Wu C T, Dai K R, et al. Proliferation and osteoblastic differentiation of human bone marrow-derived stromal cells on akermanite-bioactive ceramics. Biomaterials, 2006, 27: 5651–5657
8 Liu Q H, Cen L, Yin S, et al. A comparative study of proliferation and osteogenic differentiation of adipose-derived stem cells on akermanite and beta-TCP ceramics. Biomaterials, 2008, 29: 4792–4799
9 Huang Y, Jin X G, Zhang X L, et al. *In vitro* and *in vivo* evaluation of akermanite bioceramics for bone regeneration. Biomaterials, 2009, 30: 5041–5048
10 Ni S Y, Chou L, Chang J. Preparation and characterization of forsterite (Mg_2SiO_4) bioceramics. Ceram Int, 2007, 33: 83–88
11 Xie Y T, Zhai W Y, Chen L, et al. Preparation and *in vitro* evaluation of plasma-sprayed Mg_2SiO_4 coating on titanium alloy. Acta Biomater, 2009, 5: 2331–2337
12 Jin X G, Chang J, Zhai W Y, et al. Preparation and characterization of clinoenstatite bioceramics. J Am Ceram Soc, 2011, 94: 173–177
13 Zhu Y X, Liu T G, Song K D, et al. Adipose-derived stem cell: A better stem cell than BMSC. Cell Biochem Funct, 2008, 26: 664–675
14 Niemeyer P, Fechner K, Milz S, et al. Comparison of mesenchymal stem cells from bone marrow and adipose tissue for bone regeneration in a critical size defect of the sheep tibiaand the influence of platelet-rich plasma. Biomaterials, 2010, 31: 3572–3579
15 Lindroos B, Suuronen R, Miettinen S. The potential of adipose stem cells in regenerative medicine. Stem Cell Rev, 2011, 7: 269–291
16 Rada T, Reis R L, Gomes M E. Adipose tissue-derived stem cells and their application in bone and cartilage tissue engineering. Tissue Eng Part B-Rev, 2009, 15: 113–125
17 Yoon E, Dhar S, Chun D E, et al. *In vivo* osteogenic potential of human adipose-derived stem cells/poly lactide-co-glycolic acid constructs for bone regeneration in a rat critical-sized calvarial defect model. Tissue Eng, 2007, 13: 619–627
18 Kim A, Kim D H, Song H R, et al. Repair of rabbit ulna segmental bone defect using freshly isolated adipose-derived stromal vascular fraction. Cytotherapy, 2012, 14: 296–305
19 Leong D T, Nah W K, Gupta A, et al. The osteogenic differentiation of adipose tissue-derived precursor cells in a 3D scaffold/matrix environment. Curr Drug Discov Technol, 2008, 5: 319–327
20 Yang Z, Huang C Y, Candiotti K A, et al. Sox-9 facilitates differentiation of adipose tissue-derived stem cells into a chondrocyte-like phenotype *in vitro*. J Orthop Res, 2011, 29: 1291–1297
21 Zuk P A, Zhu M, Ashjian P, et al. Human adipose tissue is a source of multipotent stem cells. Mol Biol Cell, 2002, 13: 4279–4295
22 Liu Z Q, Wang H B, Zhang Y, et al. Efficient isolation of cardiac stem cells from brown adipose. J Biomed Biotechnol, 2010, 2010: 104296
23 Lee J H, Rhie J W, Oh D Y, et al. Osteogenic differentiation of human adipose tissue-derived stromal cells (hASCs) in a porous three-dimensional scaffold. Biochem Biophys Res Commun, 2008, 370: 456–460
24 Stiehler M, Lind M, Mygind T, et al. Morphology, proliferation, and osteogenic differentiation of mesenchymal stem cells cultured on titanium, tantalum, and chromium surfaces. J Biomed Mater Res A, 2008, 86: 448–458
25 Zuk P A, Zhu M, Mizuno H, et al. Multilineage cells from human

adipose tissue: Implications for cell-based therapies. Tissue Eng, 2001, 7: 211–228
26 Zou J, Wang G L, Geng D C, et al. A novel cell-based therapy in segmental bone defect: Using adipose derived stromal cells. J Surg Res, 2011, 168: 76–81
27 Lendeckel S, Jodicke A, Christophis P, et al. Autologous stem cells (adipose) and fibrin glue used to treat widespread traumatic calvarial defects: Case report. J Cranio-MaxilloFac Surg, 2004, 32: 370–373
28 Mesimaki K, Lindroos B, Tornwall J, et al. Novel maxillary reconstruction with ectopic bone formation by GMP adipose stem cells. Int J Oral Maxillofac Surg, 2009, 38: 201–209
29 Thesleff T, Lehtimäki K, Niskakangas T, et al. Cranioplasty with adipose-derived stem cells and biomaterial: A novel method for cranial reconstruction. Neurosurgery, 2011, 68: 1535–1540
30 Ni S Y, Chang J, Chou L. *In vitro* studies of novel CaO-SiO_2-MgO system composite bioceramics. J Mater Sci Mater Med, 2008, 19: 359–367
31 Kharaziha M, Fathi M H. Improvement of mechanical properties and biocompatibility of forsterite bioceramic addressed to bone tissue engineering materials. J Mech Behav Biomed Mater, 2010, 3: 530–537
32 Kieswetter K, Schwartz Z, Dean D D, et al. The role of implant surface characteristics in the healing of bone. Crit Rev Oral Biol Med, 1996, 7: 329–345
33 Hamidouche Z, Fromigue O, Ringe J, et al. Priming integrin alpha5 promotes human mesenchymal stromal cell osteoblast differentiation and osteogenesis. Proc Natl Acad Sci USA, 2009, 106: 18587–18591
34 Karsenty G, Wagner E F. Reaching a genetic and molecular understanding of skeletal development. Dev Cell, 2002, 2: 389–406
35 Lee H W, Suh J H, Kim H N, et al. Berberine promotes osteoblast differentiation by Runx2 activation with p38 MAPK. J Bone Miner Res, 2008, 23: 1227–1237
36 Lian J B, Stein G S. Runx2/Cbfa1: A multifunctional regulator of bone formation. Curr Pharm Des, 2003, 9: 2677–2685
37 Taubenberger A V, Woodruff M A, Bai H, et al. The effect of unlocking RGD-motifs in collagen I on pre-osteoblast adhesion and differentiation. Biomaterials, 2010, 31: 2827–2835
38 Grinnell F. Fibroblast biology in three-dimensional collagen matrices. Trends Cell Biol, 2003, 13: 264–269
39 Gordon J A, Hunter G K, Goldberg H A. Activation of the mitogen-activated protein kinase pathway by bone sialoprotein regulates osteoblast differentiation. Cells Tissues Organs, 2009, 189: 138–143
40 Wang J, Zhou H Y, Salih E, et al. Site-specific *in vivo* calcification and osteogenesis stimulated by bone sialoprotein. Calcif Tissue Int, 2006, 79: 179–189
41 Obata A, Kasuga T. Stimulation of human mesenchymal stem cells and osteoblasts activities *in vitro* on silicon-releasable scaffolds. J Biomed Mater Res A, 2009, 91: 11–17
42 Yamasaki Y, Yoshida Y, Okazaki M, et al. Action of FGMgCO_3Ap-collagen composite in promoting bone formation. Biomaterials, 2003, 24: 4913–4920
43 Zreiqat H, Valenzuela S M, Nissan B B, et al. The effect of surface chemistry modification of titanium alloy on signalling pathways in human osteoblasts. Biomaterials, 2005, 26: 7579–7586
44 Kundu A K, Khatiwala C B, Putnam A J. Extracellular matrix remodeling, integrin expression, and downstream signaling pathways influence the osteogenic differentiation of mesenchymal stem cells on poly(lactide-*co*-glycolide) substrates. Tissue Eng Part A, 2009, 15: 273–283
45 Keeting P E, Oursler M J, Wiegand K E, et al. Zeolite A increases proliferation, differentiation, and transforming growth factor beta production in normal adult human osteoblast-like cells *in vitro*. J Bone Miner Res, 1992, 7: 1281–1289
46 Zreiqat H, Howlett C R, Zannettino A, et al. Mechanisms of magnesium-stimulated adhesion of osteoblastic cells to commonly used orthopaedic implants. J Biomed Mater Res, 2002, 62: 175–184
47 Lu Z, Zreiqat H. Beta-tricalcium phosphate exerts osteoconductivity through α2β1 integrin and down-stream MAPK/ERK signaling pathway. Biochem Biophys Res Commun, 2010, 394: 323–329
48 Gu H J, Guo F F, Zhou X, et al. The stimulation of osteogenic differentiation of human adipose-derived stem cells by ionic products from akermanite dissolution via activation of the ERK pathway. Biomaterials, 2011, 32: 7023–7033